Single-shot measurement of a terahertz electric-field waveform using a reflective echelon mirror

Yasuo Minami,[a] Yusuke Hayashi, Jun Takeda, and Ikufumi Katayama
Department of Physics, Graduate School of Engineering, Yokohama National University, Yokohama 240-8501, Japan

(Received 15 May 2013; accepted 14 July 2013; published online 29 July 2013)

Single-shot measurements of terahertz (THz) electric-field waveforms are demonstrated using a reflective echelon mirror, which produces multiple probe pulses with different time-delays. The polarization rotation of the probe pulses, due to the electro-optic effect induced by the THz electric field generated from grating-coupled $LiNbO_3$, was imaged onto a two-dimensional complementary metal-oxide-semiconductor camera. A waveform with a weak peak field strength of 0.6 kV/cm was obtained with a good signal-to-noise ratio, demonstrating precise single-shot detection of the THz electric field waveform. © *2013 AIP Publishing LLC*. [http://dx.doi.org/10.1063/1.4817011]

Recently, great progress has been made in techniques for generating intense terahertz (THz) pulses. The strength of a THz electric field can exceed 100 kV/cm or even 1 MV/cm using optical rectification of wavefront-tilted laser pulses in $LiNbO_3$ with Cherenkov phase matching,[1,2] or using air plasma excitation induced by two-color laser pulses.[3] At higher frequencies (10–72 THz), electric fields on the order of GV/cm have been realized.[4] These THz pulses open new frontiers of THz science, including nonlinear spectroscopy,[5] coherent control of various physical properties such as spin precessions and antiferromagnetic spin waves,[6–8] and THz streaking of attosecond pulses.[9] Even more striking is the THz-field-induced breakdown of a substance when combined with a metamaterial,[10] which indicates the need for single-shot detection of THz pulses.

However, conventional stage-scan THz spectroscopy cannot be applied to non-repetitive phenomena, as many repeated laser pulses are required to measure a THz waveform. If simple and precise single-shot THz spectroscopy can be realized, many new applications are expected, including studies of irreversible phenomena, chaotic phenomena with shot-to-shot fluctuations and material breakdown, as well as high-speed monitoring of THz electric fields.

Some single-shot techniques have been already proposed, and each of these has advantages and disadvantages for measurements. Optical chirped pulse detection enables the single-shot detection by mapping temporal information onto each frequency spectrum,[11–15] although the time-resolution was formerly limited by the spectral resolution. Recently, the disadvantage was overcome by using sufficiently short pulsed laser, or by resolving and analyzing the interference fringes using a spectrometer with sufficiently high spectral resolution, which is successfully applied to pulse shape monitoring of the electron bunch, for example in Refs. 16–19. In the method, simpler instrumentation and signal processing are required for further spectroscopic applications. Non-collinear crossing of THz wave and a probe pulse has also been used for the single-shot detection.[20] In the method, the time window was limited to about several picoseconds, resulting in insufficient spectral resolution. Another proposed technique involves spatial separation of multiple time-delayed probe pulses using dual-transmission echelon optics.[21] The dual echelon method might be sufficiently affected by chirp coming from the echelon optics itself if one tries to use dual echelons for high-frequency detections. In addition, it is sensitively affected by the defect in elements; the echelon optics is made by quartz glass and epoxy, and the processing accuracy is normally limited to a few microns in height and a few hundred microns in width. These might lead to an obstacle in measurements.

In this work, we propose a promising method of single-shot THz detection using a reflective echelon mirror with microstructured steps on its surface.[22,23] This technique could potentially solve the above drawbacks for three reasons. First, the THz wave can be focused onto the electro-optic (EO) crystal, which leads to a sensitivity-enhancement of the THz field. Second, the probe beamlets pass through no dispersive optics, and are thus chirp-free. Third, the echelon mirror is fabricated on a nickel (Ni) block using a precise micro-machining technique, and thereby, the surface roughness is $<0.2\ \mu$m,[23] which leads to less spatiotemporal modification of probe pulses with sub-10 fs pulse duration. These advantages also enhance the signal-to-noise ratio (SNR) of the obtained THz electric field. This results in a simple and powerful method for monitoring a THz electric field on a single-shot basis.

Figure 1(a) displays the experimental setup employed in this study. We used a Ti:sapphire regenerative amplifier with 1 kHz repetition rate, 130-fs pulse duration, 1.8-mJ pulse energy, and an 800-nm center wavelength to generate and detect the THz electric field. For the generation, we used a grating-coupled x-cut $LiNbO_3$ crystal ($5 \times 5 \times 0.5\ mm^3$),[24] which has a nanoscale stripe structure of gold (Au) on the surface fabricated by electron beam lithography. A scanning electron microscope (SEM) image of the grating is shown in the inset of Fig. 1(a). The grating spacing is optimized for the first-order diffracted pulses to match the noncollinear phase matching condition in the $LiNbO_3$ crystal, as described in the following.

The relationship between incident angle α and the diffraction angle β of a grating is expressed as

$$d \sin\alpha + n_p d \sin\beta = \lambda, \quad (1)$$

[a]Email: minamiyasuo@ynu.ac.jp

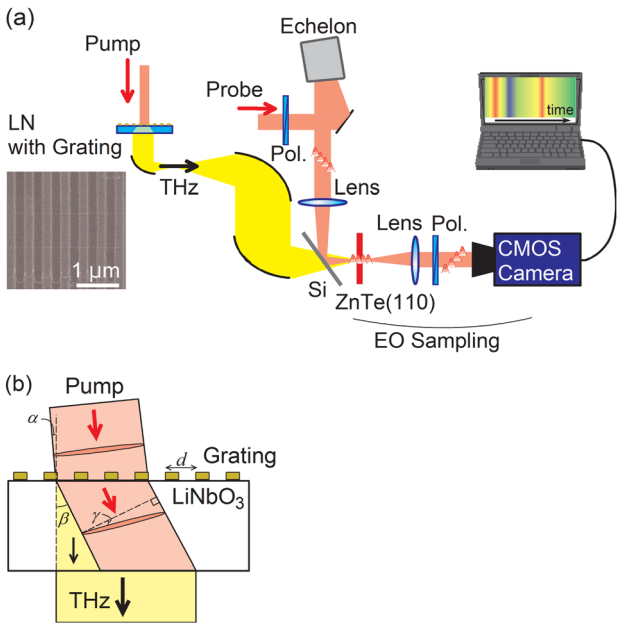

FIG. 1. (a) A schematic of single-shot detection of a THz electric field using a reflective echelon mirror. Two polarizers are arranged nearly perpendicular to each other. The inset picture is the SEM image of the grating-coupled $LiNbO_3$ crystal (LN). (b) The details of the THz generation stage.

where λ is the center wavelength of the pump beam, d is the grating spacing, and n_p is the phase refractive index of $LiNbO_3$. A schematic diagram of this geometry is displayed in Fig. 1(b). The tilted-optical-pulse front angle γ of the first-order diffracted beam at which the Cherenkov phase matching is satisfied is given by

$$n_p \tan\gamma = \frac{\sin\alpha + n\sin\beta}{\cos\beta}, \tag{2}$$

where $\gamma = \cos^{-1}(n_g/n_{THz})$, n_g is the group refractive index of $LiNbO_3$ for the pump beam at 800 nm, and n_{THz} is the phase refractive index of $LiNbO_3$ for the THz pulse at 1 THz.[25]

We chose a grating spacing of 416 nm to satisfy the above phase-matching condition to generate THz pulses with a frequency of 1 THz. Since the pump pulse can be normal to the surface ($\alpha = 0$) in this scheme, the grating-coupled $LiNbO_3$ offers a simplified method for generating THz pulses compared to the tilted-pump-pulse-front method.[1] For the detection, we used a ZnTe (110) plate with a thickness of 1 mm as an EO crystal. A reflective echelon mirror with 750 steps, whose step width and height were 20 μm and 2.5 μm, respectively, was used to produce the multiple probe beam. The probe beam diffracted from the echelon had a 17 fs time delay for each step, and an overall time delay of 13 ps. Then, we focused the probe beam on the ZnTe plate and the polarization rotation due to the THz electric field was analyzed by a nearly crossed polarizer and then imaged on a two-dimensional complementary metal-oxide-semiconductor (CMOS) camera (2560 × 2160 pixels) with 16-bit resolution. In contrast to the spectral dispersion method, the time resolution can easily be as short as the pulse duration of the probe, when the 4*f* (2*f*-2*f*) configuration is used between the echelon and the detector.

Figures 2(a) and 2(b) show the images obtained with exposure times of 5 ms (five shots) and 1 ms (single shot), respectively. The intensity contrast, shown by a color tone in Fig. 2, is due to the polarization rotation induced by the THz electric field. The horizontal direction corresponds to the time delay between the THz wave and the probe pulses. To calibrate the temporal axis, we translated the delay stage by 5 ps. As shown in Figs. 2(c) and 2(d), the peak position shifts by 943 pixels, leading to a temporal resolution of

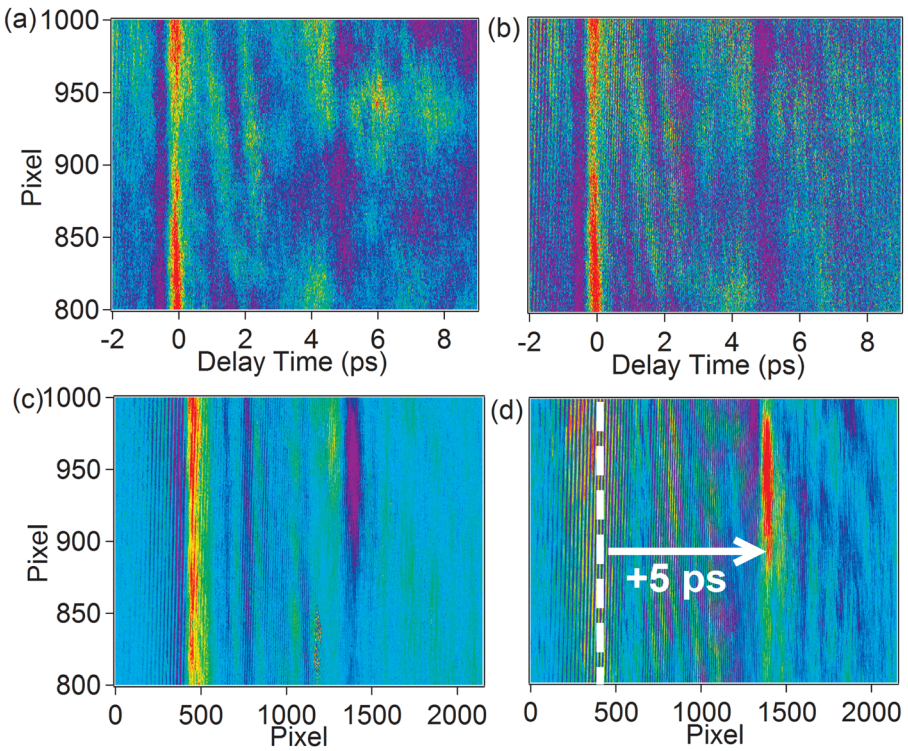

FIG. 2. Polarization rotation images of probe pulses induced by THz waves using a reflective echelon mirror: (a) five-shot measurement, (b) single-shot measurement, (c) ten-shot image before translating a delay stage (0 ps), and (d) ten-shot image after translating a delay stage (+5 ps).

5.3 fs/pixel. We used this calibration factor throughout the measurements.

Figure 3 shows (a) THz waveforms and (b) power spectra obtained using a reflective echelon mirror with five shots and a single shot. In comparison, the data measured by a conventional stage-scan method are also shown. From the conventional stage-scan method, the maximum electric field and the bandwidth of the THz wave are estimated to be 0.6 kV/cm and 0.1–2.5 THz, respectively. In the following, we will discuss the sensitivity of our single-shot detection method compared with that of the conventional stage-scan method.

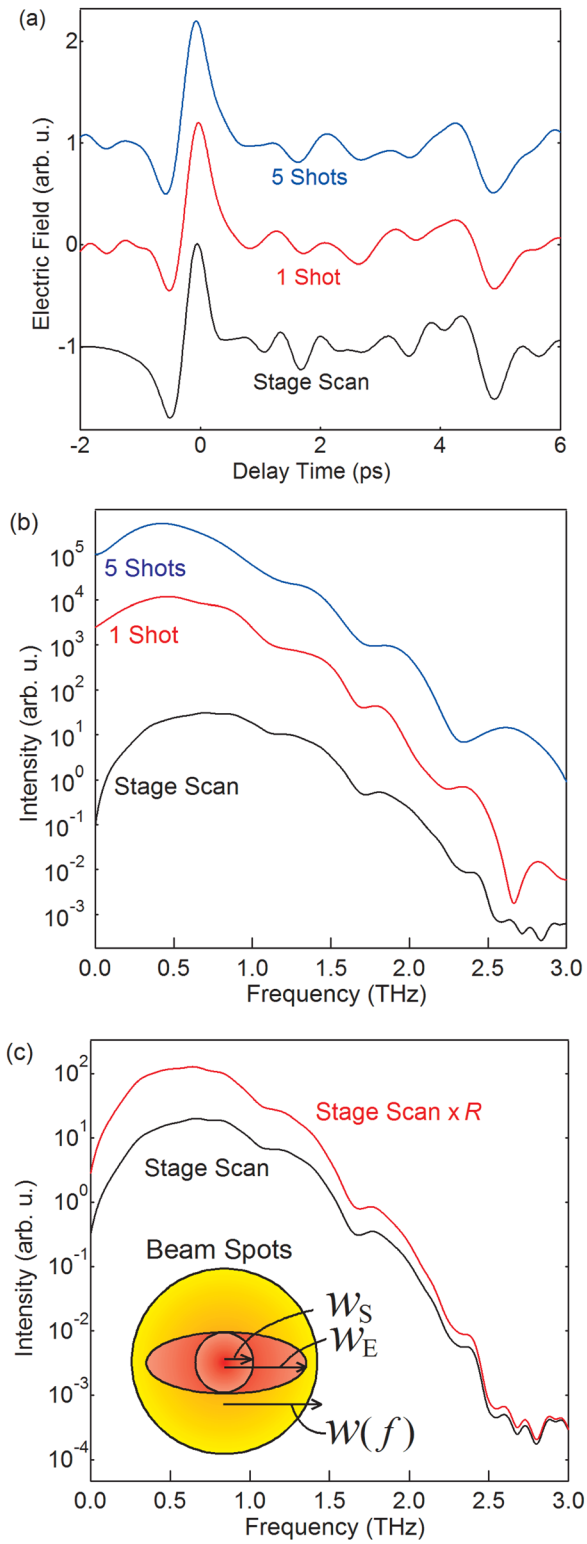

FIG. 3. (a) Observed THz electric waveforms and (b) their power spectra after Fourier transformation obtained with five shots, a single shot, and the conventional stage-scan method. (c) The power spectra obtained by the conventional stage-scan method before and after multiplication by the compensation factor R.

For the single-shot measurements, the electric field E_{THz} observed by the CMOS camera is defined by

$$E_{\mathrm{THz}}(t) \propto \frac{\lambda}{\pi L n^3 r_{41}} \left\{ \sin^{-1}\left[\sqrt{\frac{\Delta I(t)}{I}} \right] - \theta \right\}, \qquad (3)$$

where L is the thickness of the EO crystal, n is the refractive index of the EO crystal, r_{41} is the EO coefficient of the ZnTe, $\Delta I/I$ is the normalized modulation signal in EO detection, and θ is the offset angle of the second polarizer from the cross-Nicol alignment.[26] After Fourier transformation, the power spectra are obtained as shown in Fig. 3(b), in which the absorption due to water vapor is seen at 1.1 and 1.6 THz. The results demonstrate that our method can achieve a good SNR to detect comparatively weak THz signals.[27] The SNR can be improved further if the reference image is simultaneously measured for the same laser pulse, since it enables us to remove the pulse-to-pulse fluctuation in the measurement.

In Fig. 3(b), some differences between the single-shot and conventional measurements remains. To explain the differences, we estimate the effect of the beam sizes at the EO crystal. The single-shot and stage scan methods may have different waveform shapes because of the different beam sizes in the EO crystal. In the single-shot method, due to the chromatic dispersion induced by the echelon mirror, the incident angle to the focusing lens becomes non-zero and the beam spot of the probe pulse at the focus has an ellipsoidal shape whose major axis is horizontal in our setup (step direction of the echelon). The spot size at the focus in the vertical direction is the same with that of the stage scan method since the echelon has no structure in this direction. We estimated the effect of the spot shape as follows. We assumed that the spatial profiles of the THz electric field (F_{THz}) and the probe electric fields in the single-shot and stage scan methods (F_{Echelon} and F_{Stage}, respectively) at the EO crystal (or at the focus) are given by Gaussian shapes in the horizontal direction, as illustrated in the inset of Fig. 3(c). They are expressed as $F_{\mathrm{THz}} \propto \exp\left(-\frac{x^2}{w^2(f)}\right)$, $F_{\mathrm{Echelon}} \propto \exp\left(-\frac{x^2}{w_{\mathrm{E}}^2}\right)$, and $F_{\mathrm{Stage}} \propto \exp\left(-\frac{x^2}{w_{\mathrm{S}}^2}\right)$, where x is the horizontal displacement whose origin is the center of the beam, and $w(f) = \frac{cF}{\pi w_0 f}$, respectively. Here, f is the frequency of the THz beam; c is the speed of light in vacuum; $F = 100$ mm is the focal length of the parabolic mirror; and $w_0 \approx 18$ mm, $w_{\mathrm{E}} \approx 0.45$ mm, and $w_{\mathrm{S}} \approx 6.0\,\mu$m are the initial radii of the THz beam, the probe beam in the single-shot detection, and in the stage scan at the focus, respectively.

Therefore, a compensation is needed when we compare the waveform obtained from the echelon method with that from the stage scan method. The ratio of the sensitivity can be expressed as

$$R = \frac{\left(\int_0^\infty F_{\mathrm{THz}} F_{\mathrm{Echelon}} dx\right)^2}{\left(\int_0^\infty F_{\mathrm{THz}} F_{\mathrm{Stage}} dx\right)^2} \propto \left[\frac{w_{\mathrm{E}}^2}{w_{\mathrm{S}}^2} + \frac{1 - \frac{w_{\mathrm{E}}^2}{w_{\mathrm{S}}^2}}{1 + \frac{c^2 F^2}{\pi^2 w_0^2 w_{\mathrm{E}}^2 f^2}}\right]. \quad (4)$$

The spectrum obtained with the stage scan (Fig. 3(b)) is compensated as shown in Fig. 3(c). In the compensation, we set $R = 1.0$ at 3.0 THz. Note that the low-frequency THz beam is more sensitively detected in the single-shot detection than in the stage scan method. This is due to the spot size of the THz beam at the focus, in which the spot size of the low-frequency THz beam is larger than that of the high-frequency THz beam, and $w_{\mathrm{E}} > w_{\mathrm{S}}$. After compensation, the spectral shape obtained with the stage scan approaches that with the single-shot detection. Further differences might be due to the rough estimation of the spot sizes (especially w_{E}) and/or insufficient SNR of signal data taking by the single-shot measurement. In latter case, the simultaneous capture of the reference image with the signal image would improve the correspondence. This improvement is now on progress.

In conclusion, we measured the THz electric field waveform using a reflective echelon mirror on a single-shot basis. In the measurement, we obtained the precise waveforms generated from a grating-coupled $LiNbO_3$ single crystal. This method improves upon several drawbacks in previously reported single-shot measurements, and achieves a good SNR that can be feasible for spectroscopy. The results demonstrate that the single-shot technique could be a powerful tool for THz applications in the future.

This work was supported in part by the Grants-in-Aid for Scientific Research (KAKENHI, Nos. 23104713, 23241034, 23760045, 25104712, and 25800177) from JSPS.

[1]J. Hebling, G. Almási, and I. Kozma, Opt. Express **10**, 1161 (2002).
[2]H. Hirori, A. Doi, F. Blanchard, and K. Tanaka, Appl. Phys. Lett. **98**, 091106 (2011).
[3]Y. Minami, T. Kurihara, K. Yamaguchi, M. Nakajima, and T. Suemoto, Appl. Phys. Lett. **102**, 041105 (2013).
[4]A. Sell, A. Leitenstorfer, and R. Huber, Opt. Lett. **33**, 2767 (2008).
[5]I. Katayama, H. Aoki, J. Takeda, H. Shimosato, M. Ashida, R. Kinjo, I. Kawayama, M. Tonouchi, M. Nagai, and K. Tanaka, Phys. Rev. Lett. **108**, 097401 (2012).
[6]K. Yamaguchi, M. Nakajima, and T. Suemoto, Phys. Rev. Lett. **105**, 237201 (2010).
[7]T. Kampfrath, A. Sell, G. Klatt, A. Pashkin, S. Mährlein, T. Dekorsy, M. Wolf, M. Fiebig, A. Leitenstorfer, and R. Huber, Nat. Photonics **5**, 31 (2011).
[8]K. Yamaguchi, T. Kurihara, Y. Minami, M. Nakajima, and T. Suemoto, Phys. Rev. Lett. **110**, 137204 (2013).
[9]P. Del'Haye, O. Arcizet, M. L. Gorodetsky, R. Holzwarth, and T. J. Kippenberg, Nat. Photonics **3**, 529 (2009).
[10]M. Liu, H. Y. Hwang, H. Tao, A. C. Strikwerda, K. Fan, G. R. Keiser, A. J. Sternbach, K. G. West, S. Kittiwatanakul, J. Lu *et al.*, Nature **487**, 345 (2012).
[11]Z. Jiang and X.-C. Zhang, Appl. Phys. Lett. **72**, 1945 (1998).
[12]Z. Jiang and X.-C. Zhang, Opt. Lett. **23**, 1114 (1998).
[13]H. Murakami, K. Shimizu, M. Katsurada, and S. Nashima, J. Appl. Phys. **104**, 103111 (2008).
[14]K. Y. Kim, B. Yellampalle, J. H. Glownia, A. J. Taylor, and G. Rodriguez, Phys. Rev. Lett. **100**, 135002 (2008).
[15]B. Yellampalle, K. Y. Kim, G. Rodriguez, J. H. Glownia, and A. J. Taylor, Appl. Phys. Lett. **87**, 211109 (2005).
[16]J. van Tilborg, Cs. Tóth, N. H. Matlis, G. R. Plateau, and W. P. Leemans, Opt. Lett. **33**, 1186 (2008).
[17]N. H. Matlis, G. R. Plateau, J. van Tilborg, and W. P. Leemans, J. Opt. Soc. Am. B **28**, 23 (2011).
[18]Y. T. Li, C. Li, M. L. Zhou, W. M. Wang, F. Du, W. J. Ding, X. X. Lin, F. Liu, Z. M. Sheng, X. Y. Peng *et al.*, Appl. Phys. Lett. **100**, 254101 (2012).
[19]A. D. Debus, M. Bussmann, U. Schramm, R. Sauerbrey, C. D. Murphy, Zs. Major, R. Hörlein, L. Veisz, K. Schmid, J. Schreiber *et al.*, Phys. Rev. Lett. **104**, 084802 (2010).
[20]J. Shan, A. S. Weling, E. Knoesel, L. Bartles, M. Bonn, A. Nahata, G. A. Reider, and T. F. Heinz, Opt. Lett. **25**, 426 (2000).
[21]K. Y. Kim, B. Yellampalle, A. J. Taylor, G. Rodriguez, and J. H. Glownia, Opt. Lett. **32**, 1968 (2007).
[22]H. Sakaibara, Y. Ikegaya, I. Katayama, and J. Takeda, Opt. Lett. **37**, 1118 (2012).
[23]I. Katayama, H. Sakaibara, and J. Takeda, Jpn. J. Appl. Phys., Part 1 **50**, 102701 (2011).
[24]S. Sanna and W. G. Schmidt, Phys. Rev. B **81**, 214116 (2010).
[25]J. A. Fülöp, L. Pálfalvi, G. Almási, and J. Hebling, Opt. Express **18**, 12311 (2010).
[26]A. Yariv, *Quantum Electronics*, 3rd ed. (Wiley, New York, 1989), Chap. 14.
[27]T. Löffler, T. Hahn, M. Thomson, F. Jacob, and H. Roskos, Opt. Express **13**, 5353 (2005).